

SIMULATIONS OF THE LEDA RFQ 6.7-MEV ACCELERATOR *

Lloyd M. Young

Los Alamos National Laboratory, MS H817, Los Alamos, NM 87545, USA

Abstract

The codes PARMTEQM and RFQTRAK simulate the beam transport through the radio-frequency-quadrupole (RFQ) accelerator for the low-energy-demonstration accelerator (LEDA). They predict 95% transmission for a matched 110-mA proton beam with a normalized-rms emittance of 0.02 mm mrad. RFQTRAK simulates the effects of arbitrary vane-tip misalignments. This RFQ includes some new features in its design. It consists of four resonantly coupled 2-m-long segments that make up its 8-m length. It has higher vane-gap voltages at the high-energy end than the low-energy end. The entrance end of the RFQ has lower transverse focusing strength to facilitate beam matching. The exit of the RFQ has a transition cell and a radial-matching section. The exit radial-matching section matches the beam into the following accelerator.

INTRODUCTION

LEDA requires 100 mA of beam from the 350-MHz RFQ. The energy needs to be as high as possible for injection into the coupled-cavity drift-tube linac (CCDTL). Therefore, the LEDA RFQ is an 8-m-long RFQ that accelerates the proton beam to 6.7 MeV. A recent experiment with the LEDA RFQ low-power model[1] demonstrates resonantly coupling four 2-m-long segments to form an 8-m-long RFQ. The LEDA RFQ will use this configuration.

Conventional RFQ designs with a small entrance aperture require a very strongly focused beam at the entrance aperture for proper matching to the RFQ. In LEDA the final lens in the low-energy-beam transport (LEBT) is far enough from the input of the RFQ to require a large aperture and weak focusing at the beginning of the RFQ. Low vane modulation at the RFQ entrance allows weaker focusing, but still has a large transverse current limit. The combination of a large-aperture radial matching section and weak focusing makes matching the beam into the RFQ easy. As shown in Fig. 1, the transverse focusing strength smoothly increases in the first 32 cm of the RFQ. At about 130 cm, the vane gap voltage starts ramping up, the aperture starts increasing, and the focusing starts decreasing. The combination of these parameters reduces the beam loss at the end of the gentle buncher, which is the usual choke point where significant beam loss occurs.

The increase in gap voltage increases the accelerating gradient in the high-energy portion of the RFQ and shortens the length. The transverse focusing at the end of the RFQ matches the transverse focusing of the CCDTL, which makes the transition independent of the beam current.

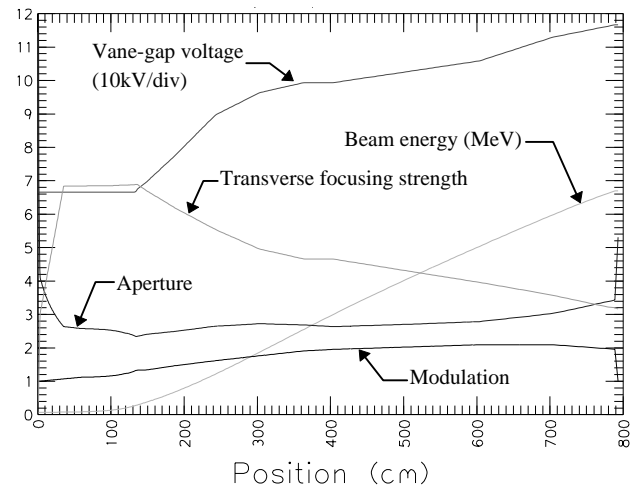


Figure 1. Shows some important parameters versus position in the RFQ.

PROGRAM RFQTRAK

RFQTRAK [2] tracks the particles through the RFQ using time as the independent variable. Particles enter a cell pair with known phase, position, and divergence angle. For each time step, RFQTRAK advances all the particles and calculates the space-charge-potential distribution. Tracking through the cell pair takes 3 RF cycles. The first cycle, which does not include space-charge fields provides the leading pulse. The third cycle provides a trailing pulse for the correct calculation of the space-charge fields. At start of the second cycle, RFQTRAK initiates the space-charge calculation. The code discards particles whose velocity falls below half the cell's synchronous velocity. Particles from the second cycle that actually exit the cell pair, provide the starting coordinates for all three cycles in the next cell pair.

RFQTRAK constructs a finite-element model of the potential distribution inside an RFQ accelerator cell. The mesh generator includes details of the topology of an RFQ cell. Mesh elements are three-dimensional bricks with 20 nodes. This number of nodes allows a quadratic variation of the potential in each dimension. The program RFQCOEF [3] calculates the first 8 multipole components of the potential in one quadrant of a single cell or optionally in all 4 quadrants of the cell. PARMTEQM [4] uses the same 8 multipole components. The 4-quadrant calculation also includes the dipole and sextupole terms.

RFQTRAK employs another finite-element mesh similar to the one used for the potential distribution to calculate the effects of space charge during the beam dynamics simulation. In this calculation, the image charge effect is naturally included by the boundary conditions. In this paper, the term space-charge effect includes the image charge effect. The finite-element model spans a pair of cells of total length $\beta\lambda$, where $\beta\lambda$ is the distance traveled

*Work supported by the US Department of Energy.

by a particle of velocity βc in one RF period. For solving Poisson's equation: $\nabla^2\Phi = -4\pi \cdot \rho$, the right-hand terms come from the beam charge distribution. The vane potentials are assigned to be zero as a boundary condition. The code maps the potential on nodes of the entrance plane to the corresponding nodes on the exit plane. A direct (Gauss Elimination) method solves for the potentials. An advantage of this method is that the solution matrix can be reused several times, with only an update of the right-hand side as the charge distribution changes. Then only a back substitution is required to solve for the fields. Space-charge fields are obtained from the potentials by differentiation of the element-shape functions.

THE SIMULATIONS

RFQTRAK simulated the LEDA RFQ with errors in the vane-tip locations and vane-tip potentials. Table 1 lists a set of randomly generated errors used in these simulations. Figure 2 shows the result of the RFQTRAK simulation with these errors. Notice that the transverse beam size shrinks in the first part of the RFQ where the focusing increases. The code RFQPROC, which is part of the PARMTEQM suite of codes, plotted all the beam distribution figures.

Table 1. Voltage and position errors for RFQ vane tips.

Vane	Voltage error (%)	Error in Vane-tip radial position (mm)	Error in vane-tip azimuthal position (mm)
1	-2.124	-0.0046	+0.0231
2	-0.159	-0.0066	-0.022
3	+3.033	+0.0017	+0.0030
4	-0.751	-0.0414	+0.040

Figure 3 shows the phase-space projections at the input of the RFQ and at the output of cell 142. The bold-black points in the input-phase-space projections are particles that were lost before reaching cell 143. At this point in the calculation, the lost particles are the outer most particles injected into the RFQ. The input beam for this simulation came from a simulation of the LEBT beam line[5]. The butterfly shape of the transverse phase-space distributions results from the large variation of the RF phase when the particles reach the cell 142-exit plane. The particles' transverse velocity at the cell exit plane depends on the RF phase.

The ellipses in these plots correspond to the rms Twiss parameters of the beam. The area is 4 times the rms emittance. The separatrix, shown in the lower right of Figure 3, defines the stable region of the phase-energy plane.

Figure 4 shows the phase space plots from the RFQTRAK simulation at cell 430, the last regular cell of the RFQ. The butterfly shape visible in the cell-142 transverse phase planes does not appear at cell 430 because the phase spread is small. Compare the RFQTRAK simulation with Figure 5, which shows the same phase-space plots from the PARMTEQM simulation. Tables 2 and 3 list the rms-beam properties of the two simulations.

The LEDA RFQ has a transition cell and a radial matching section[6]. The exit radial-matching section matches the beam into the following accelerator. PARMTEQM can simulate the transition cell and exit radial matching section, but RFQTRAK cannot. Cell 430 is the last cell where a comparison between the two codes is possible. A modification of RFQTRAK will add this capability in the near future.

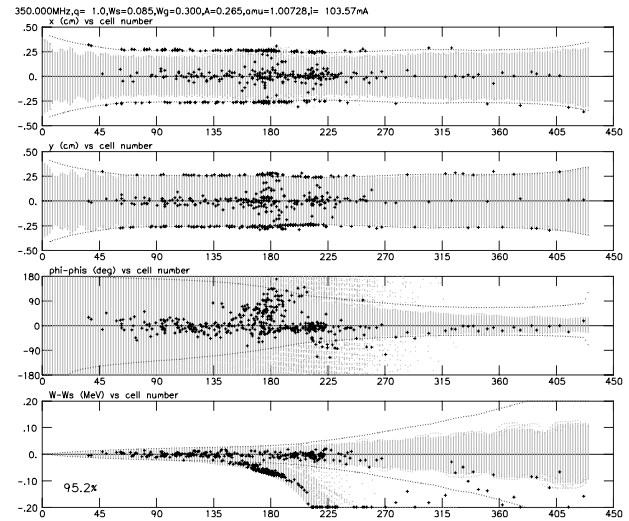


Figure 2. RFQTRAK simulated the LEDA RFQ using 100,000 macro particles. From top to bottom are: x, y, phase, and energy coordinates versus cell number. Bold-black points indicate lost particles. Only 10% of the lost particles are shown for clarity. The percentage transmission is 95.2%.

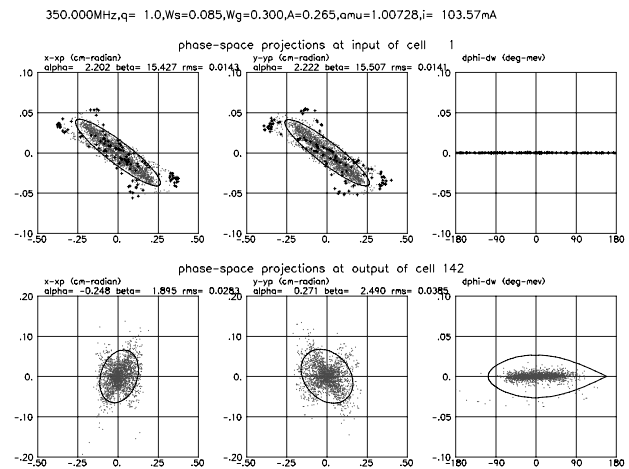


Figure 3. RFQTRAK simulation showing phase-space plots of the input beam and the beam at cell 142. Only 2% of the particles are plotted. The bold-black points in the input phase space show 10% of the particles in the input beam that have been lost up to and including cell 142. The phase-space plots from left to right are: $x-x'$, $y-y'$, and phase-energy, where $x'=dx/dz$ and $y'=dy/dz$.

PARMTEQM

PARMTEQM, which uses the z position as the independent variable and a cylindrically symmetric space-

charge calculation, cannot handle the type of errors listed in Table 1. However, PARMTEQM needs less computer resources and runs several times faster than RFQTRAK. For these reasons, we used PARMTEQM to design the LEDA RFQ. We used the PARMTEQM beam distributions to match the beam into the CCDTL. The validity of the PARMTEQM simulations can be accessed by comparing the beam distributions from PARMTEQM to the distributions from the fully 3D simulation performed in RFQTRAK.

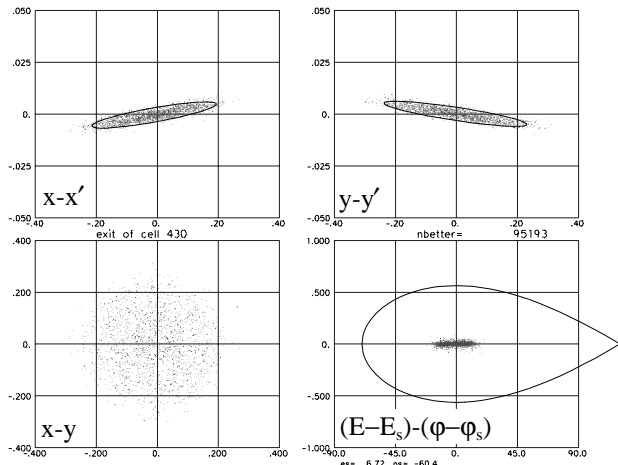


Figure 4 Phase-space projections near the end of the RFQ. Only 2% of the particles are plotted. RFQPROC calculates the Twiss parameters, α and β , and the rms emittance ϵ from the 95,193 macro particles remaining in the beam. It then draws the ellipses using $4\times\epsilon$ for the area. Table 2 lists these Twiss parameters.

Table 2. RFQTRAK Twiss parameters at cell 430.

	Twiss parameters		
Parameter	$x-x'$	$y-y'$	$(E-E_s)-(\phi-\phi_s)$
α	-1.525	1.509	0.065
β	59.02	73.48	424.4
ϵ (cm-mrad)	0.0211	0.0223	0.03407

Table 3. PARMTEQM Twiss parameters at cell 430.

	Twiss parameters		
Parameter	$x-x'$	$y-y'$	$(E-E_s)-(\phi-\phi_s)$
α	-0.750	0.591	-0.087
β	63.297	81.752	410.2
ϵ (cm-mrad)	0.0172	0.0181	0.0387

RFQTRAK calculated 95.2% transmission, which is nearly the same as 95.4% from PARMTEQM. The most significant difference between beam distributions calculated by the two codes is the difference in the emittance. In RFQTRAK the longitudinal emittance is smaller and the transverse emittance is larger. There is also a difference in the α 's and β 's. These differences are large enough that the match to the CCDTL should be checked. RFQTRAK requires the addition of the transition cell and exit radial-matching section before we can make this check. Then the PARMILA code can

transport the RFQTRAK particle distribution through the CCDTL. The results of this simulation will provide the required check of the match to the CCDTL.

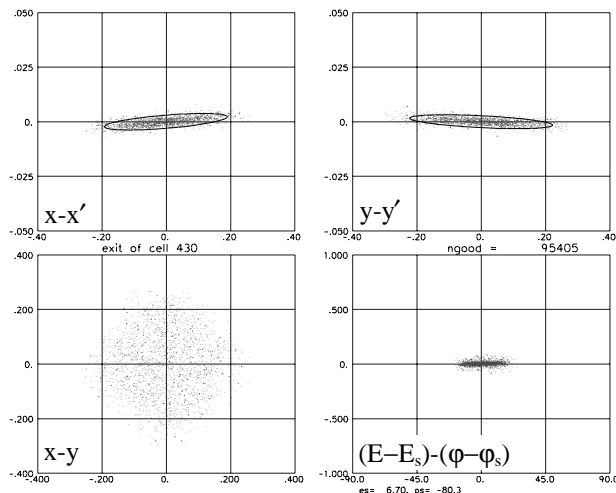


Figure 5. Phase-space projections near the end of the RFQ. Only 2% of the particles are plotted. PARMTEQM calculates the Twiss parameters, α and β , and the rms emittance ϵ from the 95,405 macro particles remaining in the beam. It then draw the ellipses using $4\times\epsilon$ for the area. Table 3 lists these Twiss parameters.

CONCLUSIONS

RFQTRAK and PARMTEQM simulations are in substantial agreement. The transmission the two codes calculate, with the same input beam, is nearly identical. There are small differences in the emittance and Twiss parameters calculated by the two codes. RFQTRAK needs further development to add the transition cell and exit radial matching section. Then PARMILA could use RFQTRAK's output beam for the CCDTL simulation.

REFERENCES

- [1] L. M. Young, "An 8-meter-long coupled cavity RFQ Linac," Proc. 1994 Intl. LINAC Conf., p. 178 (Tsukuba, Japan, Aug. 21-26, 1994).
- [2] N. J. Diserens, "Progress in the Development of a 3D finite Element Computer Program to Calculate Space and Image Charge Effects in RF Quadrupoles," IEEE Trans. Nucl. Sci., NS-32, (5), 2501 (1985).
- [3] N. J. Diserens, "RFQCOEF a Package for Extracting the Harmonic Coefficients for the Potential Function in an RF Quadrupole," Proc. 1984 Linear Accel. Conf., Darmstadt, Germany, GSI-84-11, 324 (1984).
- [4] K. R. Crandall et al., "RFQ Design Codes," Los Alamos National Laboratory report LA-UR-96-1836. (revision February 12, 1997)
- [5] L. M. Young, "Simulations of the LEDA LEBT with H^+ , H_2^+ , and e^- particles," this conference.
- [6] K. R. Crandall, "Ending RFQ Vane tips with Quadrupole Symmetry," Proc. 1994 Intl. LINAC Conf., p. 227(Tsukuba, Japan, Aug. 21-26, 1994).